Role of oxygen vacancies in room-temperature ferromagnetism in cobalt-substituted SrTiO_{3}

Chandrima Mitra, Chungwei Lin, Agham B. Posadas, and Alexander A. Demkov

Phys. Rev. B **90**, 125130 — Published 17 September 2014

DOI: 10.1103/PhysRevB.90.125130

Role of oxygen vacancies in room temperature ferromagnetism in cobalt-substituted $SrTiO_3$ – insights from first principles calculations

Chandrima Mitra, Chungwei Lin, Agham B. Posadas and Alexander A. Demkov[1a]
[a]Department of Physics, The University of Texas at Austin, Austin, TX 78712, USA

Abstract

Ferromagnetic insulating behaviour has recently been demonstrated in cobalt-substituted $SrTiO_3$ at room temperature [1]. Experimentally, it was found that a well-defined hysteresis loop only occurs at high Co concentrations of 30-40%. X-ray photoelectron spectroscopy also indicated that Co substitutes for Ti with Co being in high-spin +2 oxidation state. In this work, we employ density-functional theory to explain the experimentally observed properties of cobalt-substituted $SrTiO_3$. We examine in detail the role of oxygen vacancy (OV) defects and their formation of defect complexes with the Co ions as the origin of the ferromagnetic insulating behaviour. Our first-principles thermodynamic calculations indicate that OV defects are much more likely to occur next to Co atoms where their formation energies could be reduced by as much as 1.28 eV compared to that in bulk $SrTiO_3$. We also find that Co in these Co-OV complexes occurs in the high-spin state in agreement with core level spectroscopy, and identify a linear arrangement of the Co-OV defect complexes to be the most energetically favourable structure. These defect complexes are also shown to interact ferromagnetically and that their magnetic interaction is found to be short-ranged, consistent with the relatively high Co concentrations needed experimentally for ferromagnetism to be observed in cobalt-substituted $SrTiO_3$.

I. Introduction

The discovery of room-temperature ferromagnetism in doped transition metal oxides by Matsumoto et al. [2] has initiated many theoretical and experimental studies, owing to potential applications of these materials in spintronics. For example, ZnO [3-4], SnO_2 [5-6], In_2O_3 [7-8] and TiO_2 [9-10], have all been reported to show room-temperature ferromagnetism when doped with magnetic ions. Increasing the Curie temperature and being able to control the spin degrees of freedom remain major challenges in this field. In this respect, defects in these materials, both intrinsic and extrinsic, play an important role. Defects provide additional carriers to the system (electrons or holes) which could significantly alter magnetic interactions and the Curie temperature in these materials.

In Co-doped ZnO, for example, the role of defects in the observed room-temperature ferromagnetism was studied by several groups [11-13]. While Khare *et al.* [12] found Zn interstitials to play a crucial role in mediating ferromagnetism in Co-doped ZnO, Fonin *et. al.* [11] proposed instead that the ferromagnetic properties are strongly correlated with the presence of oxygen vacancies. Liu *et al.* [13], on the other hand, proposed the combination of Al-donor

[1] E-mail: demkov@physics.utexas.edu

and oxygen vacancy defects to be responsible for a strong carrier mediated ferromagnetic interaction in Co-doped ZnO. Transition metal-doped rutile and anatase TiO_2 are another class of oxide semiconductors that have been extensively studied for room temperature ferromagnetism [14-17]. Although, here too, defects have been proposed to enhance ferromagnetism, their exact role and the mechanism, by which they induce magnetic interactions, remain highly debatable. While interstitial Co and oxygen vacancy defects have been proposed to enhance ferromagnetism in Co-doped TiO_2 by Roberts *et al.* [16] and Weng *et. al*. [14], a ferromagnetic superexchange coupling was instead proposed by Janish *et. al.,* who did not find oxygen vacancies to play any role in the observed ferromagnetism in Co-doped TiO_2 [17].

The above-mentioned studies of magnetically doped oxide semiconductors have mainly examined dilute levels of substitution (on the order of a few percent). In more recent works, however, magnetic ions at higher doping levels have been considered in non-magnetic perovskite oxides such as $SrTiO_3$ [1,18-27]. Oxygen stoichiometry has been found to play an important role in determining the magnetic properties of these systems [18-27]. In this respect, high concentration of Co substitution in $SrTiO_3$ has been previously examined by Florez et al. [26]. They found that mixed spin states of Co^{3+} in the presence of oxygen vacancies can produce a ferromagnetic interaction between the Co atoms. However, more recent measurements of the Co oxidation state using XPS in [1] indicate that Co has a high-spin +2 valence state as indicated by the strong shake up satellite in the Co 2p core level spectrum. Additionally, it was found that Co substitution induces an amount of oxygen to be removed from $SrTiO_3$ that is roughly the same as the Co concentration, which is much higher than the amount of oxygen vacancies proposed in [26]. It was also found in [1] that a robust ferromagnetic hysteresis loop was observed only at a sufficiently high Co concentration (~30%) and that samples exhibiting ferromagnetism were highly insulating, suggesting the absence of free carriers.

The goal of the present work is to provide a theoretical understanding of the observed magnetic, spectroscopic, and electrical properties of $SrTiO_3$ that has been doped with high concentrations of Co. We investigate the role of oxygen vacancy defects in the observed valence and spin state transitions of Co. Employing density functional theory (DFT) within the local spin density approximation with Hubbard U correction (LSDA+U) [28], we first justify the likelihood of the formation of oxygen vacancies adjacent to the substituted Co atoms, forming Co-OV defect complexes. We consider different arrangements of these Co-OV defect complexes and identify the most energetically favorable structure among them. The electronic structure and the nature of magnetic interactions between these defect complexes are then studied. The paper is organized as follows. In Sections II and III we present the computational details and the electronic structure of Co-substituted STO in a defect free environment. In Section IV we introduce oxygen vacancies and critically examine their role in ferromagnetism. Our conclusions are presented in Section V.

II. Computational methods

The electronic structure of Co-substituted STO is studied within density functional theory (DFT) using the Vienna Ab-initio Simulation Package (VASP) code [29] with projector augmented wave pseudopotentials [30]. The valence electrons included for Sr, Ti and Co are $4s^2\ 4p^6\ 5s^2$, $3s^2\ 3p^6\ 4s^2\ 3d^2$, and $4s^2\ 3d^7$, respectively. A plane-wave cut-off energy of 600 eV is used. Calculations are performed on 135-atom and 40-atom supercells of $SrTiO_3$ in order to model $SrTi_{1-x}Co_xO_3$. The integrals over the Brillouin zone are performed using Monkhorst-Pack special k-point grids [31] of 4×4×4 and 6x6x6 for the 3x3x3 and 2x2x2 supercells, respectively. The energies are converged to within 10^{-6} eV/cell, and all forces are converged to within 0.004 eV/Å.

In order to take into account the correlation effects of the *d* electrons of Co, we perform LSDA+U calculations employing the simplified, rotationally invariant approach as introduced by Dudarev *et al.* [28]. In accordance with results extracted from photoemission data [32] an effective U_{eff} (where $U_{eff} = U\text{-}J$ and J=1 eV was used for all our calculations) of 4.0 eV is used for the Co *d* states. This value of U_{eff} also results in stabilizing an intermediate spin state of $2.5\mu_B$/Co in $SrCoO_3$ in agreement with experimental observations [33]. For the Ti *d* states a U_{eff} value of 8.5 eV is added in order to obtain the experimentally observed band gap of 3.2 eV in $SrTiO_3$ [34]. This high value of U_{eff} on the Ti *d* states, however, has been checked to have no effect on the magnetic moment on the Co atoms.

It is important to recognize the subtle difference in the effect of the Hubbard correction, U_{eff}, on Ti and Co d states in Co-doped STO. The key quantity is the occupation of the respective 3d orbitals. In STO, Ti occurs in a +4 valence state and therefore should nominally have zero 3d occupancy. In reality, a non-negligible contribution of Ti 3d states appears in the valence band due to hybridization with the oxygen 2p states. However, the 3d occupancy is small and the top of the valence band is mainly comprised of O-2p states, the valence band structure remains mostly unaffected even when a large value of U_{eff} is applied. It is the empty conduction band states that are shifted up, thereby increasing the band gap [35]. On the other hand, Co has nominally five (Co^{4+}) electrons in $SrTi_{1-x}Co_xO_3$ or seven (Co^{2+}) electrons in $SrTi_{1-x}Co_xO_{3-\delta}$ and the U_{eff} value can significantly affect both the spin-state and the energy of the occupied 3d levels [36]. Therefore, the choice of U_{eff} has to be consistent with the observed spin state and the valence band density of states.

III. Electronic structure of a single Co atom in STO

We first investigate the effect of a single Co atom within STO. In the absence of any defects, Co substituting a Ti site in STO should attain a valence state of +4. This means it should have 5 electrons in its outermost valence 3*d* shell. We model this by employing a 3x3x3 supercell of

STO, where a Ti atom is substituted by Co (we denote this as $SrTi_{1-x}Co_xO_3$). In order to investigate the spin state of the Co atom we plot the spin polarized partial density of states (PDOS) of Co in Fig. 1. Our calculations indicate that Co stabilizes in the low spin state of 1 μ_B/Co. As can be seen from the PDOS plot (Fig. 1), the e_g orbitals of Co are empty while the t_{2g} orbitals have a spin configuration of $[(t_{2g}\uparrow)^3(t_{2g}\downarrow)^2]$. Hence the net magnetic moment on Co sums up to 1 μ_B.

We also examine the magnetic interaction between Co atoms in $SrTi_{1-x}Co_xO_3$ by substituting two Ti atoms with Co. By comparing the total energy differences between ferromagnetic and antiferromagnetic configurations as a function of distance between the Co atoms, the strength of the magnetic interaction can be estimated. This is shown in Fig. 2. We find that ferromagnetic interaction is favored over the antiferromagnetic one by 60 meV/Co. However, the interaction is extremely short-ranged and persists only when Co atoms are present as nearest neighbors.

IV. Oxygen vacancies

Contrary to the expected +4 valence state of Co, experimental observations indicate Co to occur in the +2 valence state in Co-doped STO samples. This was confirmed by recent X-ray photoelectron spectroscopy measurements, where the Co 2*p* spectrum showed a peak at about 780.5 eV, accompanied by a strong shake up satellite feature at about 6.0 eV higher binding energy indicative of the high spin +2 valence state [1]. It is therefore imperative to consider the presence of additional carriers when describing the physics of this system. A plausible source of extrinsic carriers is oxygen vacancies (OV), which are commonly occurring defects in oxides, especially thin films. Creation of an OV in STO results in two additional electrons that can potentially convert Co from a +4 to a +2 valence state [37,38,39]. Hence understanding the role of oxygen vacancies in the observed magnetism in this system (which henceforth would be denoted as $SrTi_{1-x}Co_xO_{3-\delta}$) is crucial.

We first demonstrate if indeed, a vacancy is likely to occur near a Co atom. In order to do that, we compare the formation energy of an OV in STO for two different configurations; one where a vacancy occurs as a nearest neighbor to a Co atom (at a distance 1.92 Å from it) and another where a vacancy forms at a distance of 7Å away from Co (a 3x3x3 supercell is used). We employ the Zhang-Northrup formalism [40] where the formation energy is given by:

$$E_{form} = E_{total}(SrTi_{1-x}Co_xO_{3-\delta}) - E_{total}(SrTi_{1-x}Co_xO_3) - \mu_{O_2} \qquad (1)$$

The first two terms represent the total energy with and without the OV and μ_{O_2} is the reference chemical potential of oxygen which is chosen to be half of the binding energy of the oxygen molecule [41]. We find that E_{form} is 4.56 eV when the vacancy is placed as a nearest neighbor to Co compared to E_{form} of 5.84 eV when the vacancy is placed 7 Å away from the Co atom. This suggests that an oxygen vacancy prefers to form in the vicinity of a Co atom rather than away

from it. In the subsequent calculations, we assume the presence of a single, adjacent OV for every Co atom, and will refer to this as a Co-OV complex.

V. Spin-state of a Co-OV complex

Before investigating the spin-state of the Co-OV complex we briefly examine the structural changes induced due to the formation of this defect complex. In the absence of any defects, within the LDA+U approximation, we find the equilibrium lattice constant of $SrTiO_3$ to be 3.92 Å. In order to study the structural effects of Co-OV complex we employ a 2x2x2 supercell of $SrTi_{1-x}Co_xO_{3-\delta}$ as shown in Fig. 3(a). This corresponds to $x=\delta=0.125$. Fig. 3(b) shows a plot of the total energy as a function of the lattice constant. We find a 0.5 % reduction in the equilibrium lattice constant which now comes out to be 3.90 Å. As can be seen from Fig. 3, there also is a significant atomic rearrangement around the Co-OV defect site, particularly the Ti and the O atoms. The neighboring Ti atom, labeled *A* in the figure, moves away from the vacancy site by 0.07 Å relative to its ideal position in an unrelaxed supercell. This is in contrast to what is observed in Ti-OV-Ti, in the absence of Co, where the two Ti atoms are actually found to move closer to the vacancy site [38]. We do not find any displacement of Co from its ideal position. The four neighboring oxygen atoms, bonded to type *A* Ti, also show strong relaxation towards the vacancy site.

We now consider the electronic structure of $SrTi_{1-x}Co_xO_{3-\delta}$ for the particular configuration depicted in Fig. 3. Since an OV is an n-type defect 'donating' two electrons to the neighboring Co atom, the valence state of Co changes from a 4+ to a 2+ state. An important question is whether Co stabilizes in the High Spin (HS) or the Low Spin (LS) state. We address this by performing a "Fixed-Moment" calculation [42,43]. Freezing the net magnetic moment, on Co, to a particular spin state and subsequently performing a self-consistent calculation one can compare the energy of various spin configurations. We find that the HS state, corresponding to a magnetic moment of 3 μ_B on Co, is lower in energy by 0.4 eV/cell than the LS state corresponding to a magnetic moment of 1 μB/Co. Hence, it is expected that Co^{2+} would stabilize in the HS state in the presence of an OV. The electronic structure for both the HS and the LS states are presented in Fig. 4(a) and 4(b) respectively.

The formation of an oxygen vacancy near a Co atom breaks its octahedral symmetry and causes local hybridization of the Co 3d with its 4s and 4p states [37,38,39]. This results in splitting of both the Co t_{2g} and the e_g manifolds. In the +2 state Co has 7 valence electrons. For the HS state two of the t_{2g} states, in this case Co d_{xz} and Co d_{yz}, are fully occupied, while d_{xy} and the e_g states are partially occupied with a net magnetic moment of 3 μ_B/Co. For the LS state the t_{2g} states are all fully occupied while the e_g states are only partially filled with a net magnetic moment of 1 μ_B/Co.

VI. Magnetic interactions

In our previous work, the Co-substituted $SrTiO_3$ film grown on Si was found to exhibit a well-defined hysteresis loop only at a high concentration of Co (>20 %) [1]. The sample was also found to be under an in-plane tensile strain where the c/a ratio for $SrTiO_3$ was measured to be 0.989. In order to simulate a higher concentration of Co we had used a 2x2x2 supercell of STO. Since experimentally the valence state of Co was found to be +2 [1], for every Co atom we had introduced an OV. This corresponded to $x = \delta = 0.25$. Among the different possibilities we had identified two configurations with the lowest energies, as indicated in Fig 5(a) and 5(b). For a cubic supercell of STO, these two structures had the same ground state energy. This indicates that Co-OV complexes energetically prefer a linear arrangement. A linear clustering of vacancies and electron localization had been previously reported, where the vacancy clustering was found to decrease the vacancy mobility and to reduce the free carrier density [44].

In order to be consistent with experimental conditions we had then applied an in-plane tensile strain to the STO supercell in order to attain a c/a ratio of 0.989. Upon breaking the cubic symmetry a notable effect was the increased stabilization of the Co-OV complex within the plane of applied tensile strain (compared to the one perpendicular to it) [1]. Furthermore this configuration was found to favor a ferromagnetic alignment, compared to an antiferromagnetic one although the energy difference was only 8.0 meV/Co. Co was also in the HS state.

To further investigate the nature of magnetic interactions between Co atoms we now employ a larger supercell of STO which would allow us to consider greater number of Co-OV defect configurations. We employ a 2x2x3 supercell which has eight distinct Ti sites that could be substituted by Co. Similar to previous calculations [1], we assume an OV for every Co atom. Interestingly, in this larger supercell, the lowest energy structure also has a Co-OV defect complex arranged linearly as shown in Fig. 6(a). In Table 1 we present the energy differences between ferromagnetic and antiferromagnetic alignments of Co atoms for four different configurations of Co-OV complex. These configurations correspond to structures labeled as I, II, III and IV, as shown in Fig. 6(a) and (b). For configurations III and IV we find that both the ferromagnetic and antiferromagnetic alignments have the same energy. We were unable to stabilize an antiferromagnetic solution for configuration II (indicated by X in Table I).

We now examine the spin polarized PDOS of Co atoms for the lowest energy structure as shown in Fig. 7(a) and (b). Both Co atoms stabilize in a HS state with 3 μB/Co. For configurations I and II we find that there is an intermediate Ti atom between the two Co-OV complexes that has a small magnetic moment parallel to Co. For configuration I, which has the lowest energy, we find that one of the e_g orbitals (the d_z^2) of this Ti atom (labeled B in Fig. 8) acquires a small net spin polarization of 0.044 μ_B. This is not the case for configurations III and IV where an OV, Ti and Co atoms are not arranged in a line. The local symmetry lowering due to the vacancy causes Ti d_{z^2} to mix with Ti 4s and 4p orbitals making a spatially extended hybrid orbital approximately 1

eV lower than the bulk state [35]. In structure I, this state overlaps with the Co state of similar nature. This lowers the overall energy and results in Ti acquiring a small moment.

It is now instructive to comment briefly on the effect of the Hubbard parameter on the Ti d states and how this correction could affect our magnetic calculations. A U_{eff} value of 8.5 eV was used to obtain the experimentally observed band gap of 3.2 eV in STO. It also resulted in an equilibrium lattice parameter of 3.92 Å, which is a slight overestimation from the experimental value of 3.905 Å. Upon applying U_{eff} on Ti d, the empty conduction Ti d states are pushed up while the relative ordering of the occupied Ti d states (within the valence bands) with respect to the O p states is also expected to be somewhat modified. It is therefore necessary to carefully examine the effect of the Hubbard correction on the magnetic results. In order to do so we repeat our calculations (comparing the energy differences between a ferromagnetic and an antiferromagnetic configuration) for U_{eff}=0 and U_{eff}=3 eV. We present these results in Table 1. As can be seen, we find a consistent trend for all the values of U_{eff} used. We therefore believe that the qualitative conclusions of our work will remain the same, irrespective of the value of U_{eff} used.

VII. Conclusions

We have performed a first principles theoretical analysis of Co substitution in STO in the presence of oxygen vacancies, in order to investigate the role of these vacancies in the observed room temperature ferromagnetism of cobalt-substituted STO. We find that oxygen vacancies transform the valence state of Co from the expected 4+ to 2+ by donating two electrons to it. The Co-OV complex is found to be thermodynamically stable and a linear arrangement of such complexes is energetically favored. In-plane tensile strain is found to preferentially stabilize the Co-OV complex to lie along one of the in-plane directions, which is important in strained epitaxial films. Co^{2+} is found to occur in the high-spin state in the presence of an OV. A very short-range ferromagnetic interaction between the Co-OV defect complexes is predicted for the linear configuration. This is in line with the experimental observations where ferromagnetism in the Co-doped STO samples is found to occur only at high concentrations of Co (>25%) [1].

Acknowledgments

Support for this work was provided through Scientific Discovery through Advanced Computing (SciDAC) program funded by U.S. Department of Energy, Office of Science, Advanced Scientific Computing Research and Basic Energy Sciences under award number DESC0008877, Office of Naval Research under Grant No. N000 14-10-1-0489, and Texas Advanced Computing Center.

References

[1] A. Posadas, C. Mitra, C. Lin, A. Dhamdhere, D. J. Smith, M. Tsoi, and A. A. Demkov, Phys. Rev. B **87**, 144422 (2013).

[2] Y. Matsumoto, M. Murakami, T. Shono, T. Hasegawa, T. Fukumura, M. Kawasaki, P. Ahmet, T. Chikyow, S. Koshihara, and H. Koinuma, Science **291**, 854 (2001).

[3] C. Song, K. W. Geng, F. Zeng, X. B. Wang, Y. X. Shen, F. Pan, Y. N. Xie, T. Liu, H. T. Zhou, and Z. Fan, Phys. Rev. B **73**, 024405 (2006).

[4] K. Ueda, H. Tabata and T. Kawai , Appl. Phys. Lett. **79**, 988 (2001).

[5] H. S. Kim, L. Bi, G. F. Dionne, C. A. Ross and H. J. Paik, Phys. Rev. B **77**, 214436 (2008).

[6] S. B. Ogale, R. J. Choudhary, J. P. Buban, S. E. Lofland, S. R. Shinde, S. N. Kale, V. N. Kulkarni, J. Higgins, C. Lanci, J. R. Simpson, N. D. Browning, S. Das Sarma, H. D. Drew, R. L. Greene, and T. Venkatesan, Phys. Rev. Lett. **91**, 077205 (2003).

[7] J. Philip, A. Punnoose, B. I. Kim, K. M. Reddy, S. Layne, J. O. Holmes, B. Satpati, P. R. Leclair, T. S. Santos and J. Moodera, Nat. Mater. **5**, 298 (2006).

[8] Y. K. Yoo, Q. Xue, H.-C. Lee, S. Cheng, X.-D. Xiang, G. F. Dionne, S. Xu, J. He, Y. S. Chu, S. D. Preite, S. E. Lofland, and I. Takeuchi, Appl. Phys. Lett. **86**, 042506 (2005).

[9] K. A. Griffin, A. B. Pakhomov, C. M. Wang, S. M. Heald and K. M. Krishnan, Phys. Rev. Lett. **94**, 157204 (2005).

[10] S.A. Chambers, C. M. Wang, S. Thevuthasan, T. Droubay, D. E. McCready, A.S. Lea, V. Shutthanandan and C. F. Windisch, Jr., Thin Solid Films 418, 197 (2002).

[11] M. Fonin, G. Mayer, E. Biegger, N. Janben, M. Beyer, T. Thomay, R. Bratschitsch, Y. S. Dedkov and U. Rüdiger, J. Phys.: Conf. Ser. **100,** 042034 (2008).

[12] N. Khare, M. J. Kappers, M. Wei, M. G. Blamire, and J. L. MacManus-Driscoll, Adv. Mater. **18**, 1449 (2006).

[13] E. Liu, Y. He and J. Z. Jiang, Appl. Phys. Lett. **93**, 132506 (2008).

[14] H. M. Weng, X. P. Yang, J. M. Dong, H. Mizuseki, M. Kawasaki, and Y. Kawazoe, Phys. Rev. B **69**, 125219 (2004).

[15] J. M. Sullivan and S. C. Erwin, Phys. Rev. B **67**, 144415 (2003).

[16] K. G. Roberts, M. Varela, S. Rashkeev, S. T. Pantelides, S. J. Pennycook, and K. M. Krishnan, Phys. Rev. B **78**, 014409 (2008).

[17] R. Janisch and N. A. Spaldin, Phys. Rev. B **73**, 035201 (2006).

[18] D. H. Kim, L. Bei, P. Jiang, G. F. Dionne, and C. A. Ross, Phys. Rev. B **84**, 014416 (2011).

[19] L. Bi, H.-S. Kim, G. F. Dionne, and C. A. Ross, New J. Phys. **12**, 043044 (2010).

[20] C. Pascanut, N. Dragoe, and P. Berthet, J. Magn. Magn. Mater. 305, 6 (2006).

[21] C. Decorse-Pascanut, J. Berthon, L. Pinsard-Gaudart, N. Dragoe, and P. Berthet, J. Magn. Magn. Mater. 321 3526 (2009).

[22] S. Malo and A. Maignan, Inorg. Chem. 43, 8169 (2004).

[23] P. Galinetto, A. Casiraghi, M. C. Mozazti, C. B. Azzoni, D. Norton, L.A. Boatner, and V. Trepakov, Ferroelectrics 368, 120 (2008).

[24] D. Yao, X. Zhou, and S. Ge, Appl. Surf. Sci. 257, 9233 (2011).

[25] G. F. Dionne, J. Appl. Phys. **101**, 09C509 (2007).

[26] J. M. Florez, S. P. Ong, M. C. Onbaşli, G. F. Dionne, P. Vargas, G. Ceder, and C. A. Ross, Appl. Phys. Lett. **100**, 252904 (2012).

[27] S. X. Zhang, S. B. Ogale, Darshan C. Kundaliya, L. F. Fu, N. D. Browning, S. Dhar,W. Ramadan, J. S. Higgins, R. L. Greene et al., Appl. Phys. Lett. 89, 012501 (2006).

[28] S. L. Dudarev, G. A. Botton, S. Y. Savrasov, C. J. Humphreys, and A. P. Sutton, Phys. Rev. B **57**, 1505 (1998).

[29] G. Kresse and J. Furthmüller, Phys. Rev. B **54**, 11169 (1996).

[30] P. E. Blöchl, Phys. Rev. B **50**, 17953 (1994).

[31] H. J. Monkhorst and J. D. Pack, Phys. Rev. B **13**, 5188 (1976).

[32] A. Y-C. Yu and W. E. Spicer, Phys. Rev. **167**, 674 (1968).

[33] Y. Long, Y. Kaneko, S. Ishiwata, Y. Taguchi, and Y. Tokura, J. Phys. Condens. Matter **23**, 245601 (2011).

[34] K. van Benthem and C. Elsässer, J. Appl. Phys. **90**, 6156 (2011).

[35] J.Lee and A.A. Demkov, Phys. Rev. B **78**, 193104 (2008)

[36] H.Seo, A. Posadas and A. A. Demkov, Phys. Rev. B **86**, 014430 (2012).

[37] C. Lin, C. Mitra, and A. A. Demkov, Phys. Rev. B **86**, 161102(R), (2012).

[38] C. Mitra, C. Lin, J. Robertson, and A. A. Demkov, Phys. Rev. B **86**, 155105 (2012).

[39] C. Lin and A.A. Demkov Phys. Rev. Lett. **111**, 217601 (2013).

[40] S. B. Zhang and J. E. Northrup, Phys. Rev. Lett. **67**, 2339 (1991).

[41] R. O. Jones and O. Gunnarsson, Rev. Mod. Phys. **61**, 689 (1989).

[42] A. R. Williams, V. L. Moruzzi, J. Kübler and K. Schwartz, Bull. Am. Phys. Soc. 29, 278 (1984).

[43] K. Schwartz and P. Mohn, J. Phys. F **14**, L129 (1984).

[44] D. D. Cuong, B. Lee, K. M. Choi, H.-S. Ahn, S. Han, and J. Lee, Phys. Rev. Lett. **98**, 115503 (2007)

Tables

Table I: energy difference between the antiferromagnetic and ferromagnetic alignment for different configurations indicated in Fig. 6 for different values of *U* on Ti d states.

Configurations	**E_{AFM}-E_{FM} (meV) [U_{eff} = 8.5 eV]**	**E_{AFM}-E_{FM} (meV) [U_{eff} = 3 eV]**	**E_{AFM}-E_{FM} (meV) [U_{eff} = 0]**
I	10	15	15
II	X	X	X
III	0	0	0
IV	0	0	0

Figure Captions

Fig. 1: Orbital-resolved local density of states of the Co atom in $SrTi_{1-x}Co_xO_3$ for x = 0.037.

Fig 2: Energy difference between the antiferromagnetic and ferromagnetic alignment of two Co atoms as first, second, and third nearest neighbors. The ferromagnetic alignment is preferred only for the first nearest neighbor configuration.

Fig 3(a): A 2x2x2 supercell of $SrTi_{1-x}Co_xO_{3-\delta}$ (x = δ = 0.125) showing a Co-OV complex.

Fig 3(b): Total energy as a function of the lattice constant of $SrTi_{1-x}Co_xO_{3-\delta}$ (x = δ = 0.125).

Fig. 4(a) 2x2x2 supercell of $SrTi_{1-x}Co_xO_{3-\delta}$ with Co-OV pairs oriented along the x-axis and (b) oriented along z-axis.

Fig 5: 2x2x3 supercells of Co-substituted STO containing a pair of Co-OV complexes. I, II, III and IV represent different Co-Vac defect arrangements.

Fig. 6: Orbital-resolved PDOS of two Co atoms corresponding to the lowest energy structure (configuration I).

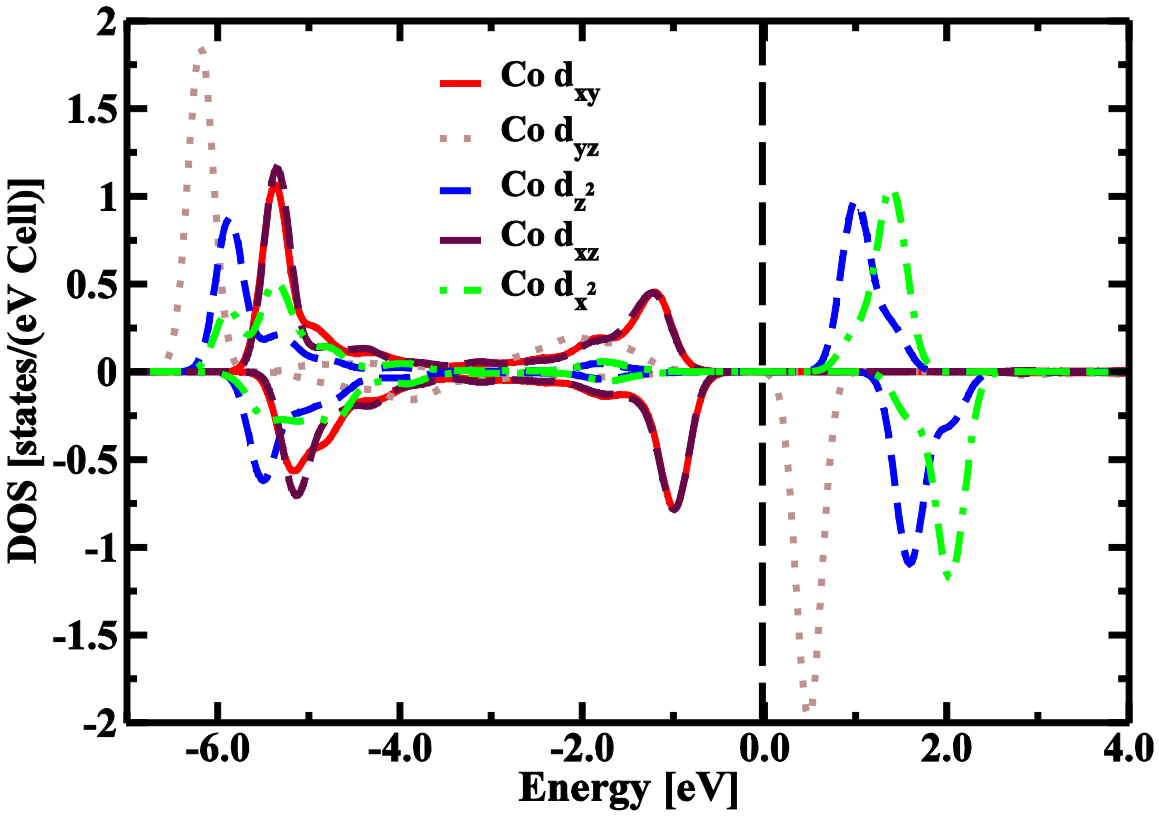
Co d$_{xy}$
Co d$_{yz}$
Co d$_{z^2}$
Co d$_{xz}$
Co d$_{x^2}$
DOS [states/(eV Cell)]
Energy [eV]
2
1.5
1
0.5
0
-0.5
-1
-1.5
-2
-6.0
-4.0
-2.0
0.0
2.0
4.0

Fig. 1

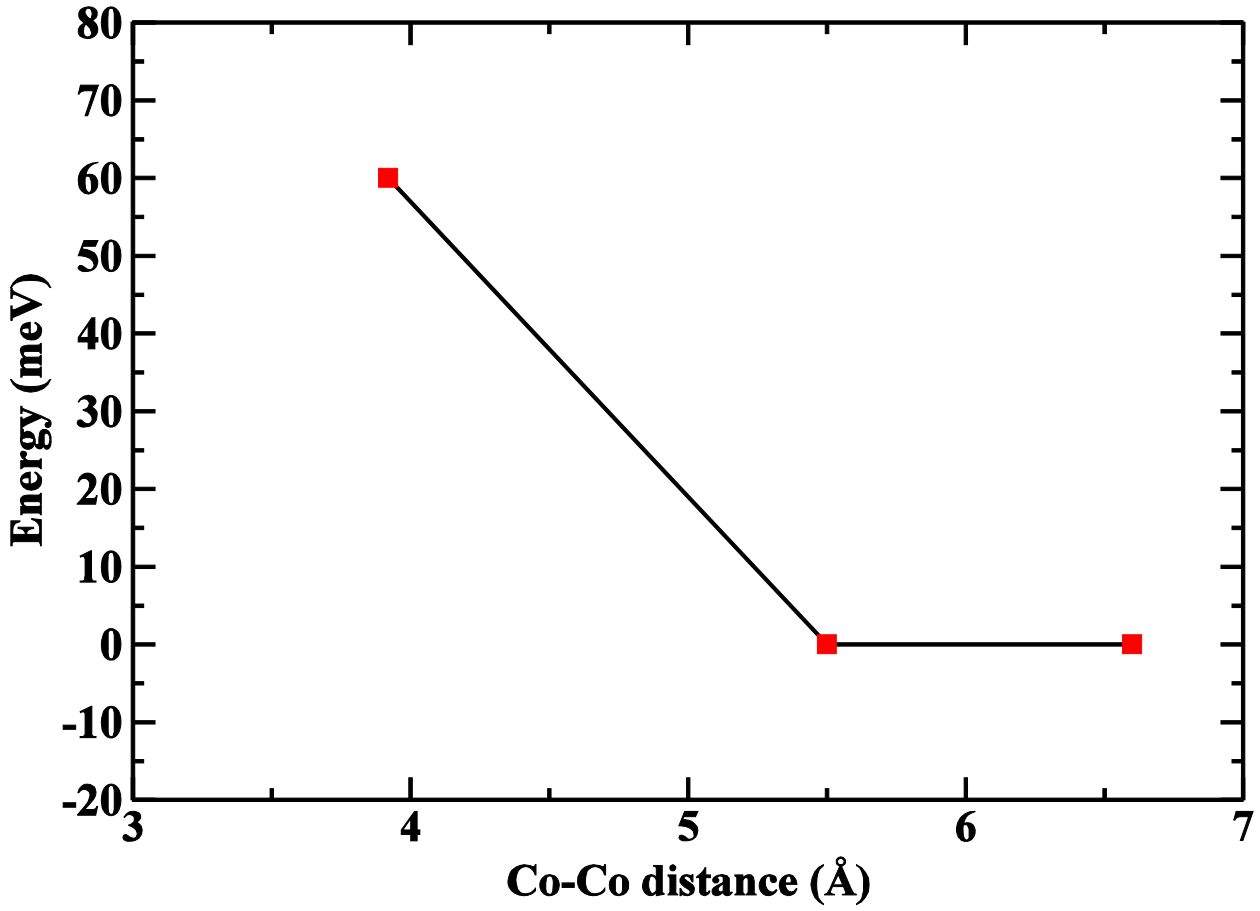

Fig. 2

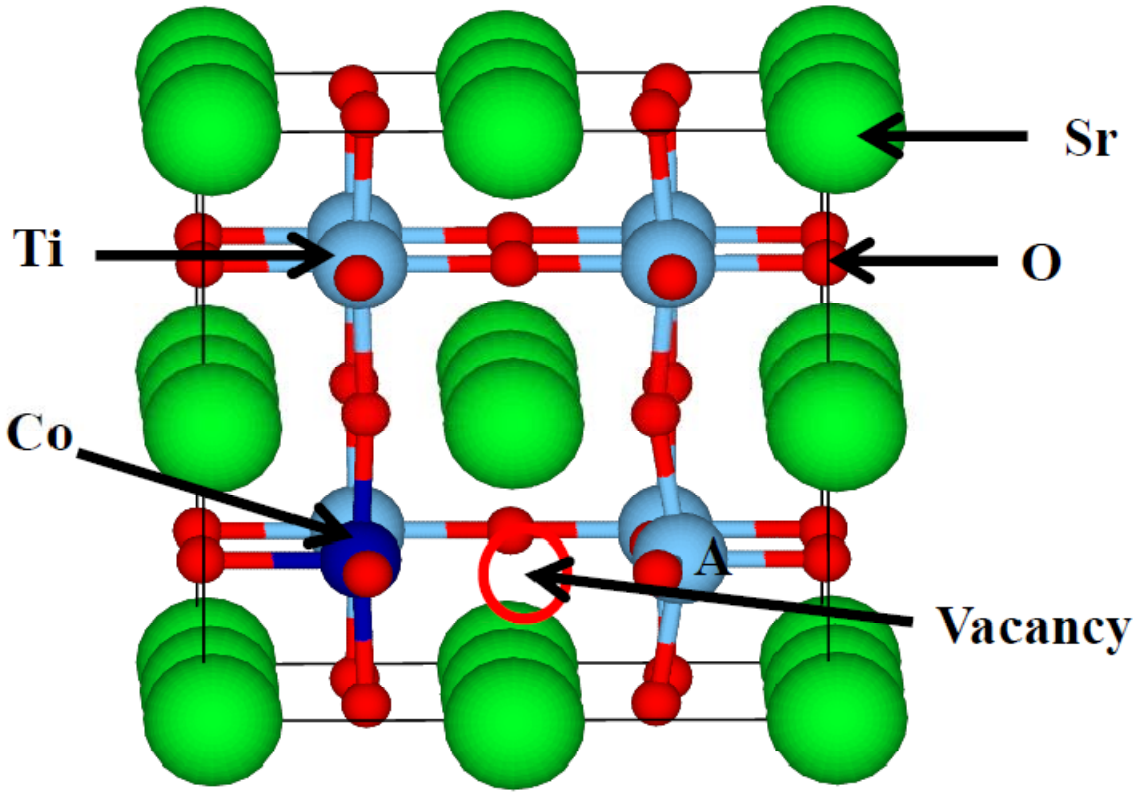

Fig. 3 (a)

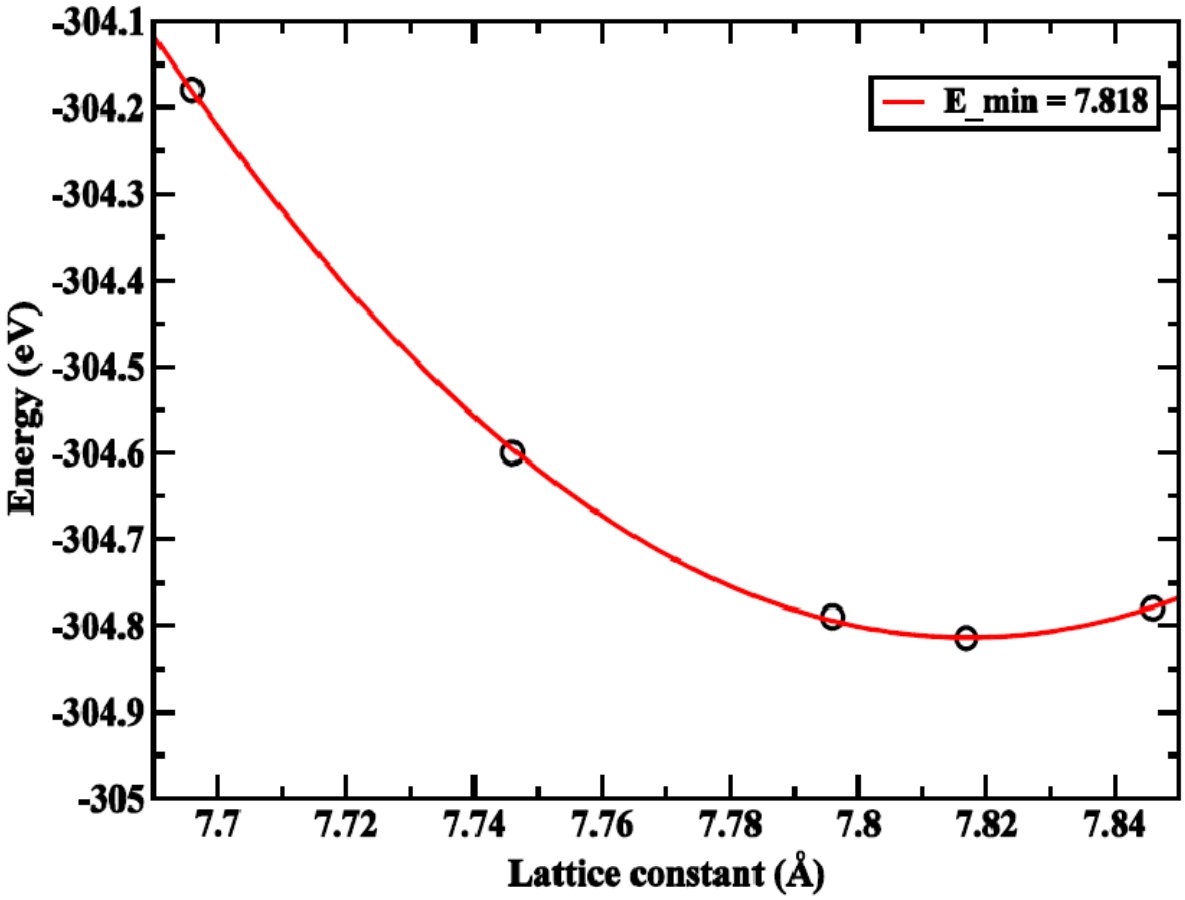
E_min = 7.818
Energy (eV)
-304.1
-304.2
-304.3
-304.4
-304.5
-304.6
-304.7
-304.8
-304.9
-305
7.7
7.72
7.74
7.76
7.78
7.8
7.82
7.84
Lattice constant (Å)

Fig. 3(b)

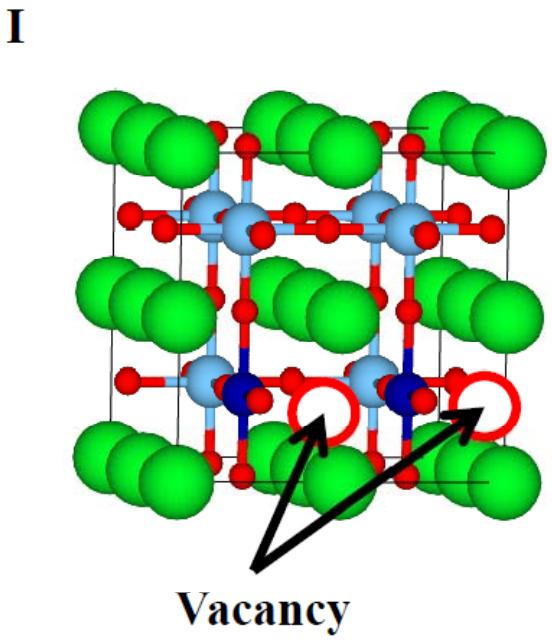

Fig. 4(a)

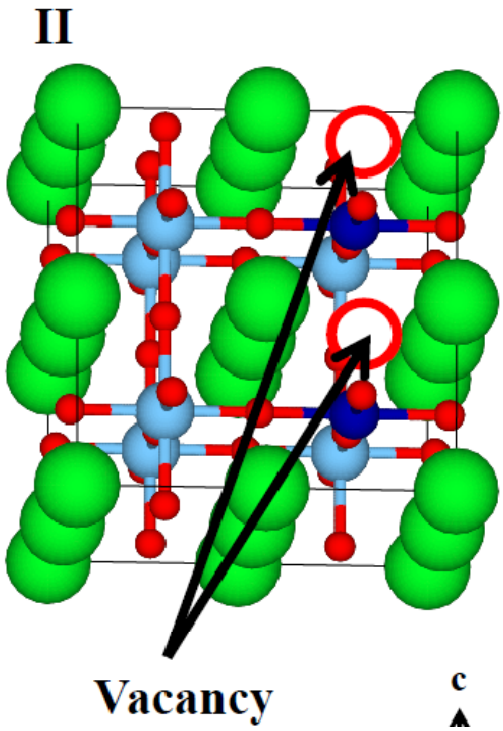

Fig. 4(b)

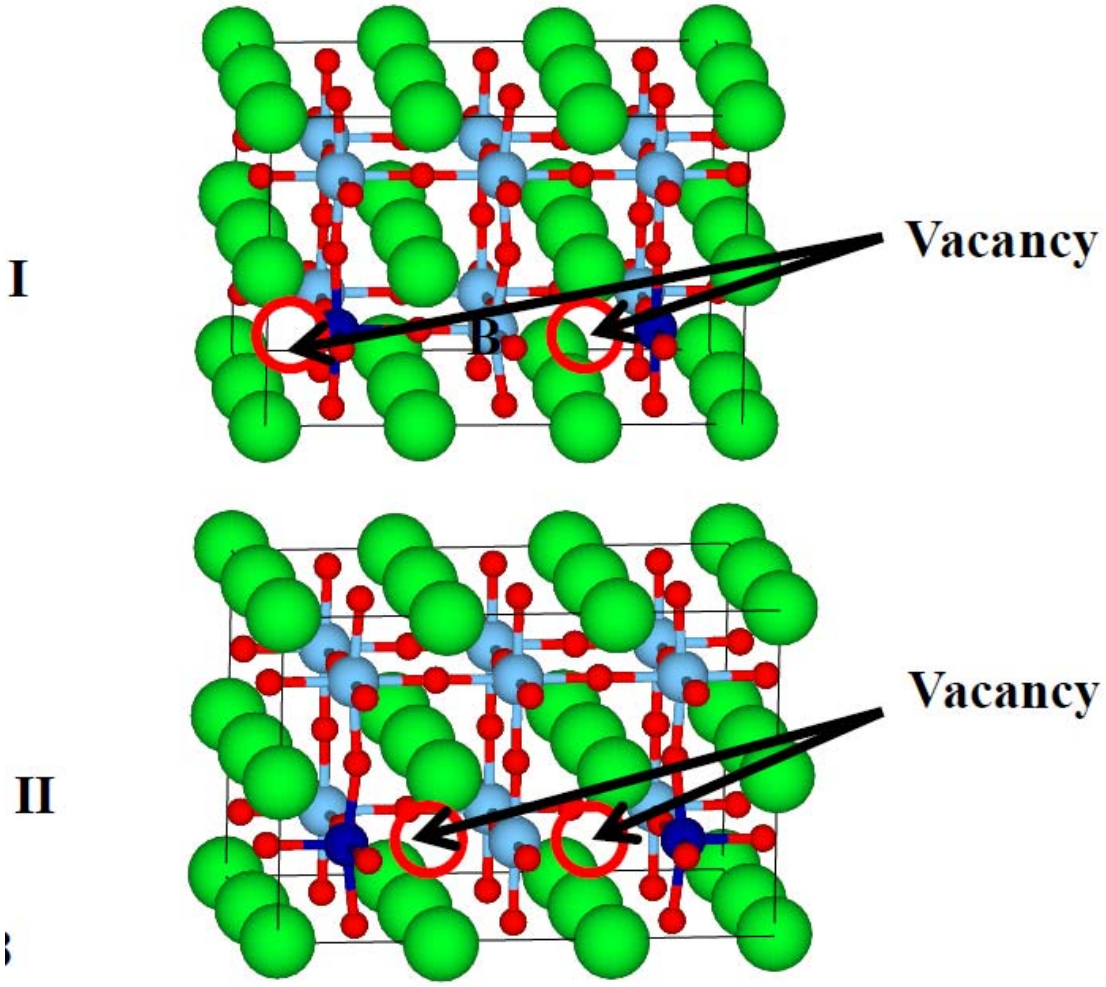

Fig. 5 (a)

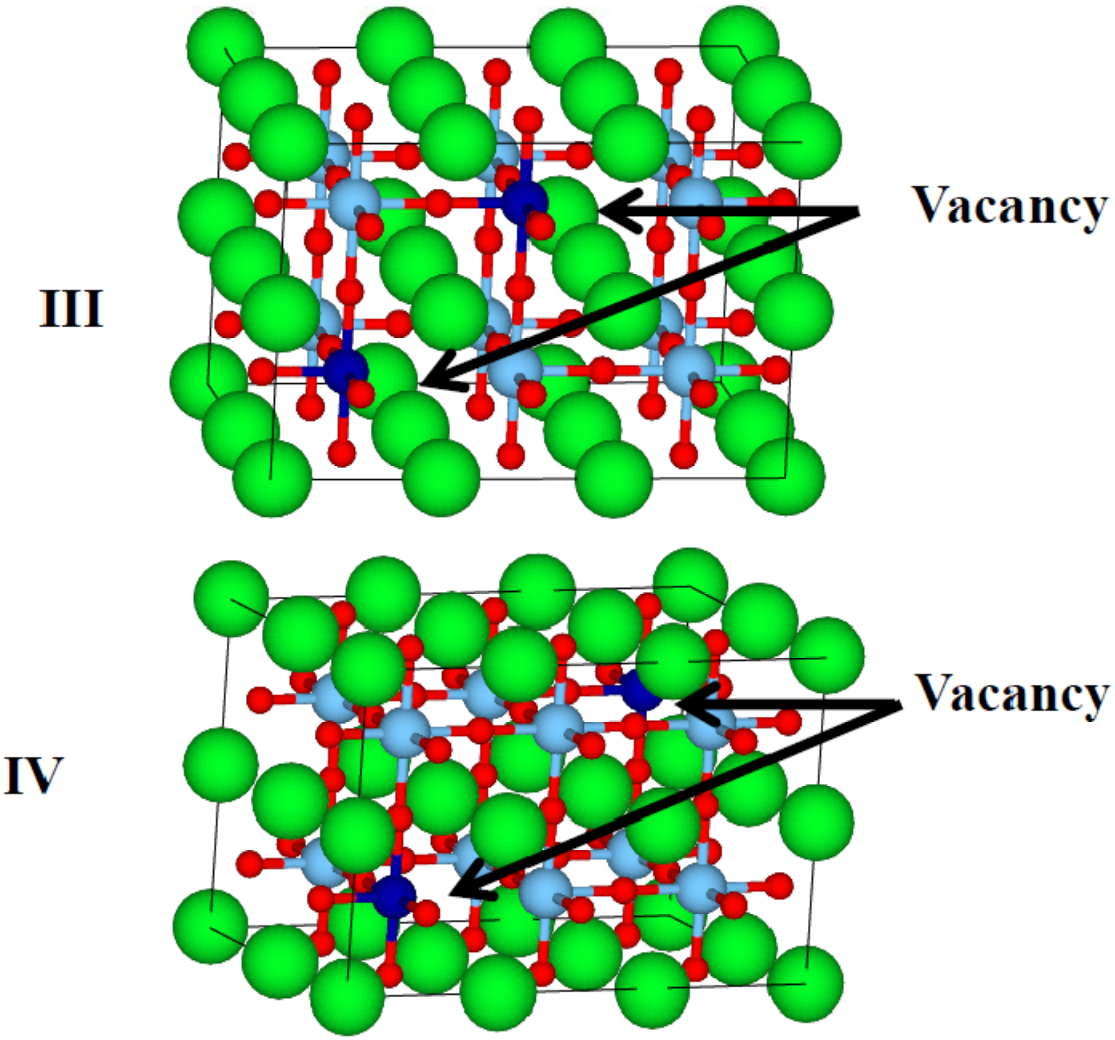

Fig. 5(b)

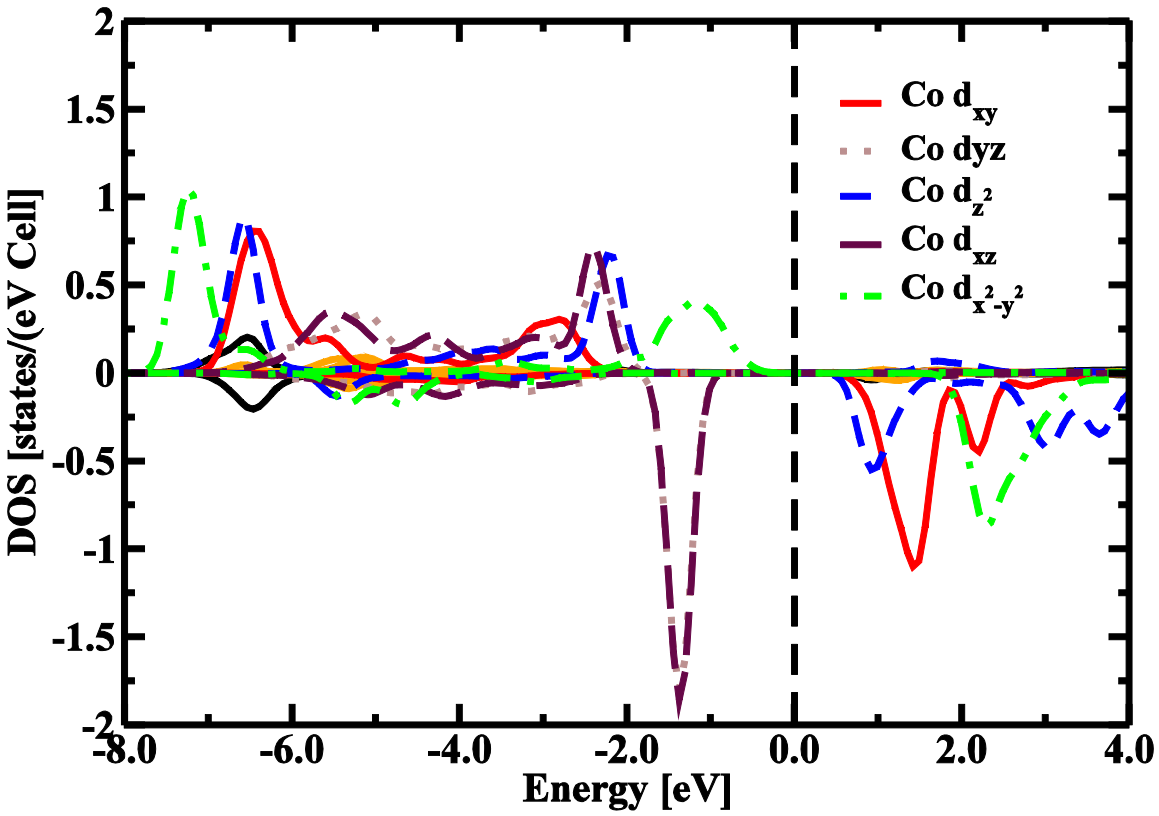
DOS [states/(eV Cell]
Energy [eV]
Co d$_{xy}$
Co dyz
Co d$_{z^2}$
Co d$_{xz}$
Co d$_{x^2-y^2}$
2
1.5
1
0.5
0
-0.5
-1
-1.5
-2
-8.0
-6.0
-4.0
-2.0
0.0
2.0
4.0

Fig. 6(a)

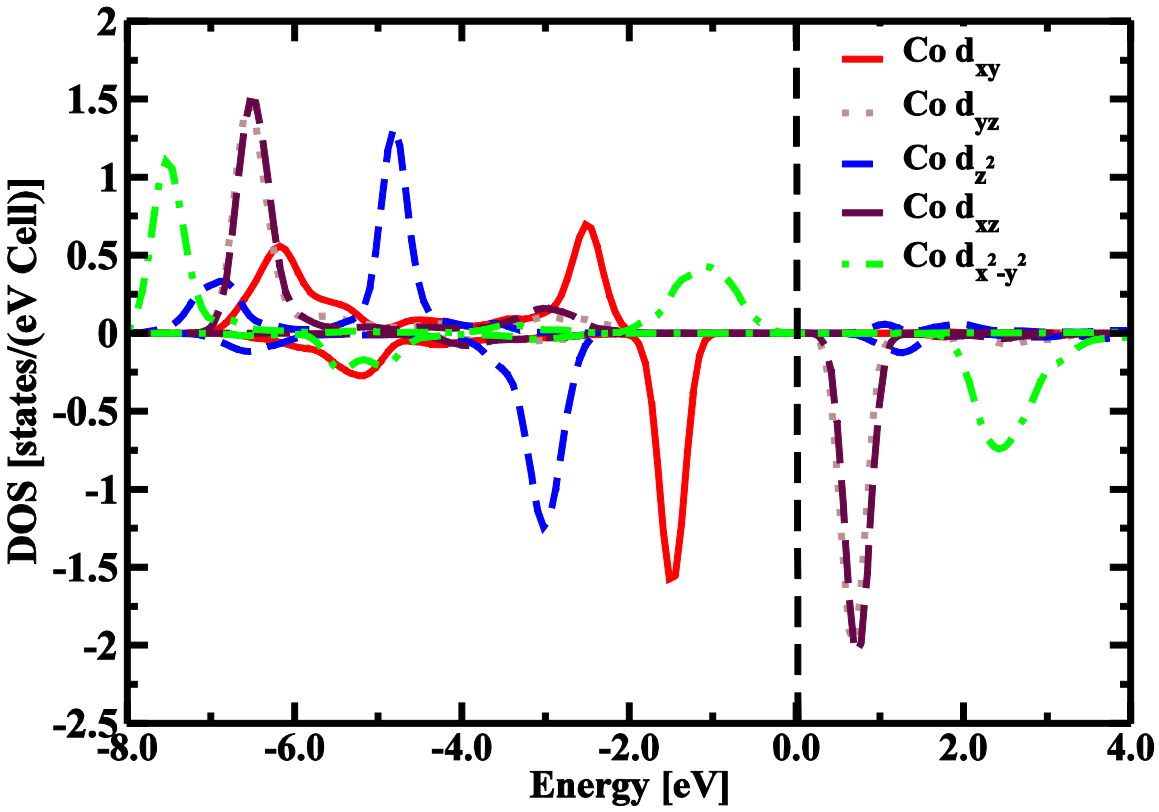
Co d$_{xy}$
Co d$_{yz}$
Co d$_{z^2}$
Co d$_{xz}$
Co d$_{x^2-y^2}$
DOS [states/(eV Cell)]
Energy [eV]
2
1.5
1
0.5
0
-0.5
-1
-1.5
-2
-2.5
-8.0
-6.0
-4.0
-2.0
0.0
2.0
4.0

Fig. 6(b)